Available online at www.sciencedirect.com
ScienceDirect
Journal of Power Sources 165 (2007) 916–921
JOURNAL OF POWER SOURCES
www.elsevier.com/locate/jpowsour

Short communication

Effect of synthesis conditions on characteristics of the precursor material used in NiO·OH/Ni(OH)$_2$ electrodes of alkaline batteries

M.B.J.G. Freitas [a,*], R.K. Silva e Silva [a], D.M. Anjos [b], A. Rozário [a], P.G. Manoel [b]

[a] *Universidade Federal do Espírito Santo, CCE, DQUI, Laboratório de Eletroquímica Aplicada, Av. Fernando Ferrari s/n, Goiabeiras, CEP 29060-900 Vitória-ES, Brazil*

[b] *Universidade de São Paulo, IQ-DEM, Av. Dr. Carlos Botelho 1465, Caixa Postal 359, CEP 13560-970 São Carlos, Brazil*

Received 10 September 2006; received in revised form 10 November 2006; accepted 17 November 2006
Available online 25 January 2007

Abstract

The synthesis of nickel hydroxide occurs by many stages. When the precipitating reagent is NH_4OH solution, the precipitation of nickel hydroxide occurs between pH 8.0 and 8.6. For pH between 8.6 and 10.0, a soluble complex such as $[Ni(NH_3)_6]^{2+}$ is formed. The precipitation of nickel hydroxide happens again after the pH equals 10.0. Finally, there occurs the ageing of α-Ni(OH)$_2$. A mixture of α-Ni(OH)$_2$ and β-Ni(OH)$_2$ phases is formed when the solid state reaction is not totally completed. One adsorbed layer becomes very hard with the exit of the water intercalated in the α-Ni(OH)$_2$. In presence of KOH solution occurs the formation and the ageing of α-Ni(OH)$_2$. Synthesis was characterized by the following techniques: X-ray diffraction, Fourier transform infrared spectroscopy (FT-IR), differential thermal analysis (DTA) and gravimetric thermal analysis (GTA), and specific surface area and UV–vis spectroscopy.

Keywords: Alkaline batteries; Chemical synthesis; Precipitation

1. Introduction

There is substantial scientific and technological interest in the study of nickel hydroxide synthesis due to its application in the positive electrodes of alkaline batteries. The NiO·OH/Ni(OH)$_2$ electrodes constitute the positive plates of nickel–iron, nickel–cadmium, nickel–zinc, nickel–hydrogen and nickel–metal hydride batteries [1,2]. Nickel hydroxide can be formed as α-Ni(OH)$_2$ or β-Ni(OH)$_2$ phases. In the α-Ni(OH)$_2$ lattice, intercalated water molecules and alkali metal ions separate the (0 0 1) plane. The lattice parameters for unit cell in the hexagonal system are $c_o = 8.05$ Å and $a_o = 3.08$ Å. The α-Ni(OH)$_2$ is unstable in the presence of alkali and on ageing, it becomes β-Ni(OH)$_2$. The ageing process consists of transformation of α-Ni(OH)$_2$ in β-Ni(OH)$_2$, by water and alkali metal ion elimination [3–5]. Due to α-Ni(OH)$_2$ instability in alkaline solutions, β-Ni(OH)$_2$ is frequently used as a precursor material in the alkaline battery. Lattice parameters for β-Ni(OH)$_2$ in the hexagonal system are $c_o = 4.65$ Å and $a_o = 3.12$ Å. The process of synthesis of the precursor material is still not fully understood. Microstructural control of the nickel hydroxide is being researched to improve the performance of the NiO·OH/Ni(OH)$_2$ electrode [6–10]. The presence of α-Ni(OH)$_2$ in the precursor material increases the specific capacity of the NiO·OH/Ni(OH)$_2$ electrodes [11]. In this work, a study of the relationship between the chemical synthesis and the microstructure of the nickel hydroxide was performed. The materials and the chemical process were characterized in different stages of preparation through the following techniques: X-ray diffraction, Fourier transform infrared spectroscopy (FT-IR), differential thermal analysis (DTA), gravimetric thermal analysis (GTA), and specific surface area and UV–vis spectroscopy.

2. Experimental

The reagents used in this synthesis method for precipitation of the nickel hydroxide were: (A) 2KOH 1.0 mol l^{-1} + $NiSO_4$ 1.0 mol l^{-1} and pH 10, (B) 2KOH 1.0 mol l^{-1} + Ni(NO$_3$)$_2$ 1.0 mol l^{-1} and pH 10, (C) 2NH_4OH 1.0 mol l^{-1} + Ni(NO$_3$)$_2$ 1.0 mol l^{-1} and pH 10, (D) 2NH_4OH 1.0 mol l^{-1} + Ni(NO$_3$)$_2$

* Corresponding author. Tel.: +55 27 33352486; fax: +55 27 33352460.
E-mail address: marcosbj@hotmail.com (M.B.J.G. Freitas).

0378-7753/$ – see front matter © 2006 Elsevier B.V. All rights reserved.
doi:10.1016/j.jpowsour.2006.11.026

0.1 mol l^{-1} and pH 10, (E) 2NH_4OH 1.0 mol l^{-1} + $Ni(NO_3)_2$ 0.1 mol l^{-1} and pH 8 and (F) 2NH_4OH 1.0 mol l^{-1} + $NiSO_4$ 1.0 mol l^{-1} and pH 10.

2.1. Synthesis of nickel hydroxide

The synthesis was carried out as follows: KOH or NH_4OH solutions were added by dripping into the nickel solution at a rate of 10.0 ml min^{-1}. The suspension was constantly stirred. The addition of reagent solution ceased when the pH was equal to 8 (synthesis E) or 10 (synthesis A, B, C, D and F). When the addition of the reagent was complete, the digestion process began and proceeded for 24 h. After that, the precipitate was washed in order to remove the excess reagent ions. The separation between the precipitate and the solution was done by centrifugation at 1500 rpm for 50 min. In the synthesis A and F, an aliquot was removed from the upper solution after sedimentation of the precipitate. $BaCl_2$ 1.0 mol l^{-1} in excess was added to the solution, causing the precipitation of $BaSO_4$. The washing of the precipitate was concluded when a white precipitate of $BaSO_4$ was not found in the wash water. This approach was adopted to conclude the washing operation. This operation was repeated five times, on average. In the other syntheses, because of the high solubility of the nitrate, it was not possible to make any visual test to determine the end of the washing operation. Therefore, after sedimentation, the pH of the upper solution was monitored and the precipitate formed was washed five times. In the next stage, the precipitate was dried at 50 °C for 72 h. The nickel hydroxide mass remained constant in these conditions. Finally, the precipitate was pulverised and the powder was passed through a 37-mesh sieve.

2.2. Characterization techniques

The X-ray diffraction powder patterns of the samples were carried out with a Rotaflex-Rigaku model 200B diffractometer. Cu Kα radiation (λ = 1.5418 Å) was used. The scan speed was 2° min^{-1} in 2θ. The Fourier transformation infrared spectroscopy was measured on a Bomem model 102 spectrophotometer with KBr pellets in the interval between 400 and 4000 cm^{-1}. DTA and GTA were performed by means of a thermal meter Netzsch model STA 409. Specific surface area was obtained by the BET adsorption method using a surface analyzer ASAP model 2000 V-2.04. UV–vis spectroscopy of the nickel solutions were made with the help of a Cary model. The centrifuging of the nickel hydroxide precipitate was done with a centrifugal Fek Brake model Top M03.

3. Results and discussion

3.1. Precursor material characterization

Typical examples of X-ray diffraction for nickel hydroxide are shown in Fig. 1. In comparison with JCPDS cards [12,13] verified that β-$Ni(OH)_2$ was formed in the synthesis A, B, D, E and F. Mixtures of α-$Ni(OH)_2$ and β-$Ni(OH)_2$ were formed in the synthesis C. This demonstrates that, the ageing process where α-$Ni(OH)_2$ becomes β-$Ni(OH)_2$ was not totally completed. The thickness of the crystallites, normal to the (0 0 1) diffraction plane was calculated with Scherrer's equation and the value found was between 40.0 and 50.0 nm. The enlargement of the diffraction peaks occurred due to the small size of crystallites and the badly crystallized precursor material.

Table 1
Absorption in the Fourier transformation infrared spectroscopy

Wave number (cm^{-1})	Attributions	Synthesis
3638	Vibrational stretching of hydroxyl group in the nickel hydroxide lattice,	A B C D E F
3427	Stretching vibrational of hydroxyl group of the adsorbed water	A B C D E F
1636	Water angular deformation	A B C D E F
569	Water angular deformation in plane	A B C D E F
386	Water angular deformation outside-of-plane	A B C D E F
448	Ni–O vibrational stretching	A B C D E F
2424, 2356	CO_2 present in the air	A B C D E F
1121, 1069	Sulphate anion	A F
1384, 998	Nitrate anion	B C D E
1382, 1025 (shoulder)	Carbonate anion	A C

FT-IR spectra prove that on the crystallite surface of the nickel hydroxide powder synthesised by methods A, B, C, D, E and F there are retained anions from the mother solution. FT-IR spectra also have characteristic bands of adsorbed and intercalated water molecules [14]. The absorption bands for nickel hydroxide synthesised by method A, B, C, D, E and F can be seen in Table 1.

In Fig. 2 shows a typical thermogravimetric plot for $Ni(OH)_2$ synthesised by methods A, B, C, D, E and F. The percentage of relative mass loss is plotted against the temperature increase. There are two temperature intervals where significant mass loss can be detected. The first one is the interval between 40 and 250 °C that corresponds to the elimination of adsorbed water for beta nickel hydroxide and adsorption and intercalated water for alpha/beta nickel hydroxide. The second is the range between 250 and 450 °C that corresponds to the reaction: $Ni(OH)_2 \rightarrow NiO + H_2O$ and the desorption of anions [15,16]. NiO calcination happened in the temperature range between 450 and 700 °C, before the beginning of powder sintering. Quantitative analysis was made with previous knowledge of the following data: the initial values of nickel hydroxide mass and the relative water loss in the interval between 40 and 250 °C. The fraction between the amount of substance (mol) of water and $Ni(OH)_2$ was determined. Chemical compositions for nickel hydroxide are in agreement with gravimetric thermal analysis, X-ray diffraction and infrared spectroscopy measurements as can be seen in Table 2.

The relation between the specific surface area and the synthesis method is shown in Table 2. In this table, it can be observed that the high amount of water on the power and the nitrogen adsorption lead to the formation of van der Waals' interactions and hydrogen bonding. These short-range interactions provoke the association of the particles

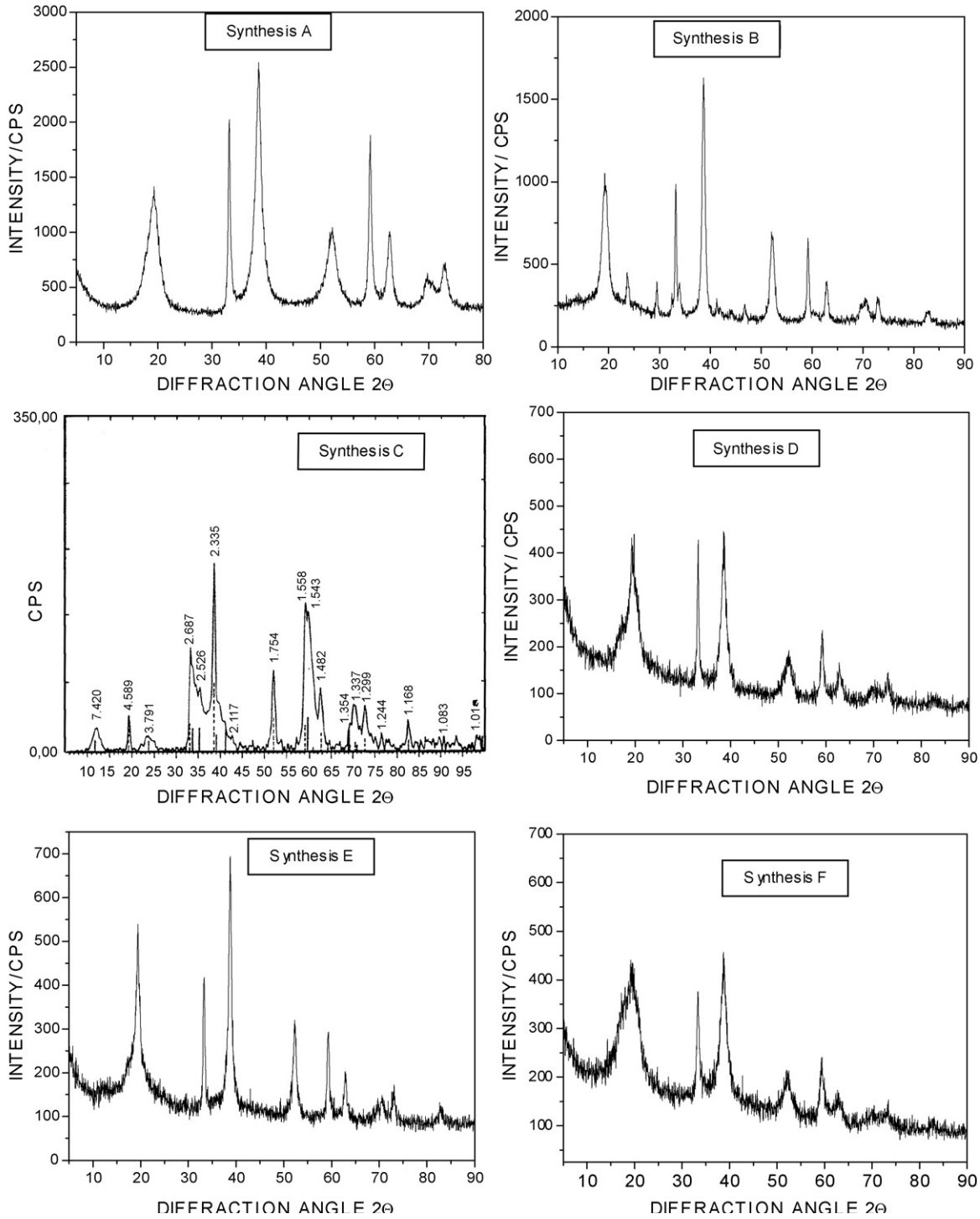

Fig. 1. X-ray diffraction pattern for nickel hydroxide synthesized for the methods A, B, C, D, E and F.

forming agglomerates and decreasing the specific surface area.

3.2. Mechanism for precursor material formation

In the syntheses A and B, beta nickel hydroxide was obtained independent of the composition of the nitrate or sulphate anions. The alpha nickel hydroxide phase is stabilized when the synthesis of the precursor material is carried out under the C conditions. In the routes D, E and F, only beta nickel hydroxide was obtained. With decrease of the concentration of nitrate (synthesis D) and pH (synthesis E), the speed of the ageing of the alpha phase in beta nickel hydroxide happens more quickly than in C. The formation of a mixture of α-$Ni(OH)_2$ and β-$Ni(OH)_2$ can be attributed to the adsorption of the nitrate anion on the solid surface. The adsorbed layer on the solid became very hard due to the

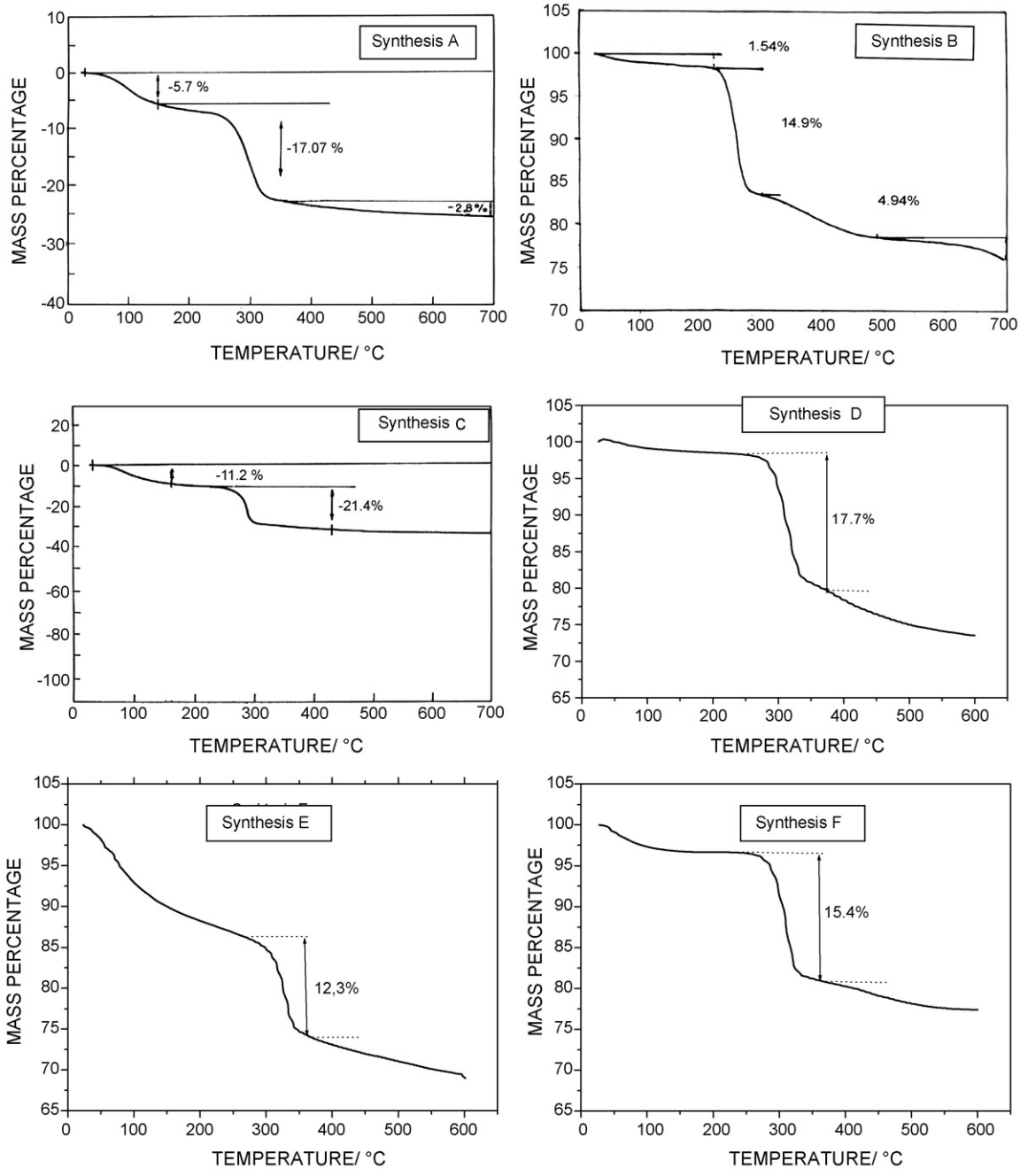

Fig. 2. Thermogravimetric plot for nickel hydroxide synthesized for the methods A, B, C, D, E and F, temperature scans of the 7 °C min^{-1}.

Table 2
Characteristics of the nickel hydroxide powder

Synthesis	Chemical composition	Specific surface area ($m^2 g^{-1}$)
A	$[\beta\text{-}Ni(OH)_x(H_2O)_{0.30}(SO_4)_y(CO_3)_{2-x-2y/2}]$	114.0
B	$[\beta\text{-}Ni(OH)_x(H_2O)_{0.081}(NO_3)_z]$	110.0
C	$[\alpha/\beta\text{-}Ni(OH)_x(H_2O)_{0.65}(NO_3)_z(CO_3)_{2-x-z/2}]$	35.5
D	$[\beta\text{-}Ni(OH)_x(H_2O)_{0.13}(NO_3)_z]$	28.8
E	$[\beta\text{-}Ni(OH)_x(H_2O)_{0.73}(NO_3)_z]$	25.7
F	$[\beta\text{-}Ni(OH)_x(H_2O)_{0.46}(SO_4)_y]$	24.8

exiting of water intercalated in the α-$Ni(OH)_2$. Adsorbed layers of nitrate anions on the solid decrease with the decrease of the $NO_3{}^{-1}$ concentration and pH. This was verified in the syntheses D and E. Therefore, for alpha nickel hydroxide, there is an optimal condition that depends on the NH_4OH and $Ni(NO_3)_2$ concentration and pH. In the presence of NH_4OH and $Ni(SO_4)$, the phase beta is stable as shown in synthesis F. This confirms that the anion adsorption delays the ageing process. Due to the complexity of the problem, more work is required to clarify the effects of these variables on the products. But, it was verified that the composition of the solution used in the synthesis does have an influence in the microstructure of the precursor

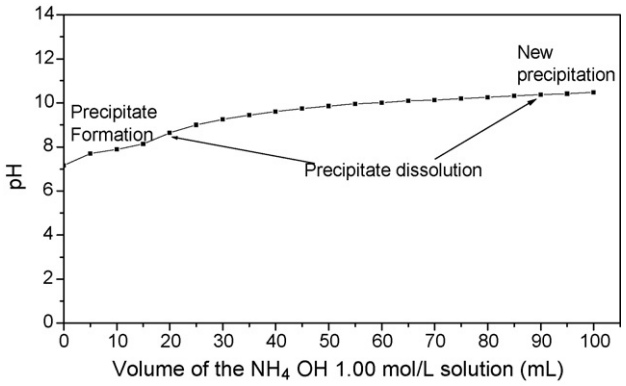

Fig. 3. Typical pH change with the addition of the NH_4OH 1.0 mol l^{-1} in the $Ni(NO_3)_2$ 0.1 mol l^{-1} solution, synthesis D, temperature of 298 K.

material. When NH_4OH is used as a precipitant reagent the synthesis occurs in many stages. The first one is the precipitation of the nickel hydroxide in pH between 8.0 and 8.6. The second, in pH between 8.6 and 10.0, is the formation of a complex as $[Ni(NH_3)_6]^{2+}$. The precipitation of the nickel hydroxide happens again after pH 10.0. Finally, occurs a solid-state reaction. Fig. 3 shows a typical variation of the pH during the synthesis. UV–vis spectroscopy was used to monitor this reaction mechanism as can be seen in Fig. 4. The adsorption peak of the Ni^{2+} solution at 393 nm decrease for 366 nm when it is formatted to $[Ni(NH_3)_6]^{2+}$. Another peak at 366 nm corresponds to the spin-orbit coupling effects that alter the energies of the orbital. The mechanism for precursor material formation in NH_4OH solution can be expressed as follows:

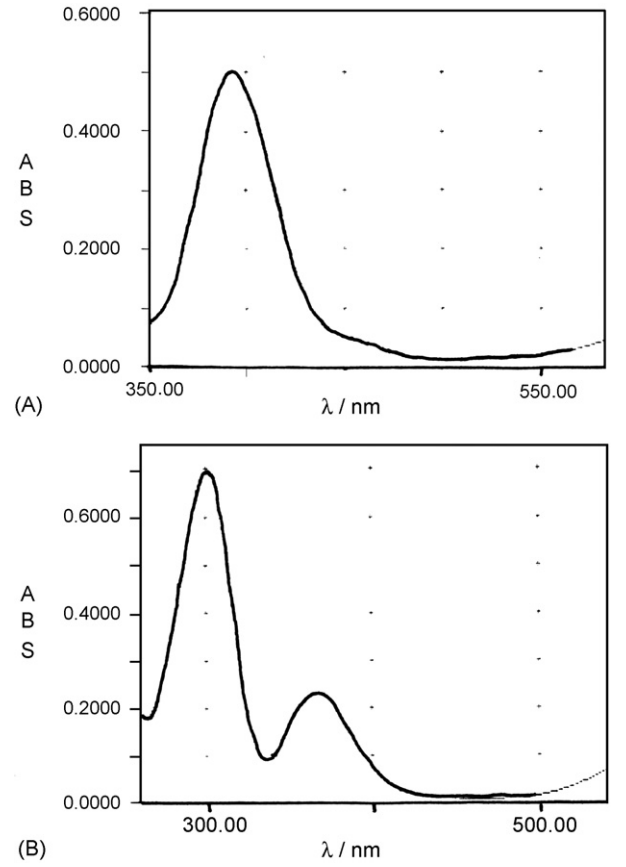

Fig. 4. UV–vis spectroscopy of the: (A) Ni^{2+} solution and (B) $[Ni(NH_3)_6]^{2+}$ solution.

1. $Ni^{2+}_{(aqueous)} + 2OH^-_{(aqueous)} \rightarrow \alpha\text{-}Ni(OH)_{2(solid)}$
2. $\alpha\text{-}Ni(OH)_{2(solid)} \rightarrow \beta\text{-}Ni(OH)_{2(solid)}$
3. $\beta\text{-}Ni(OH)_{2(solid)} + 6NH_{3(aqueous)} \rightarrow [Ni(NH_3)_6]^{2+}_{(aqueous)} + 2OH^-_{(aqueous)}$
4. $[Ni(NH_3)_6]^{2+}_{(aqueous)} + 2OH^-_{(aqueous)} \rightarrow \alpha\text{-}Ni(OH)_{2(solid)} + 6NH_{3(aqueous)}$
5. $\alpha\text{-}Ni(OH)_{2(solid)} \rightarrow \beta\text{-}Ni(OH)_{2(solid)}$

The ageing process (stage 2 or 5) is slower in synthesis C than in syntheses D, E and F. Therefore, a mixture of α-$Ni(OH)_2$ and β-$Ni(OH)_2$ phases is formed. This behaviour can be attributed to the adsorption of the nitrate anion on the solid surface. The adsorbed layer on the solid became very hard from the exit of the water intercalated in the α-$Ni(OH)_2$.

The mechanism for the precursor material formation in KOH solution is:

1. $Ni^{2+}_{(acuoso)} + 2OH^-_{(acuoso)} \rightarrow \alpha\text{-}Ni(OH)_2$
2. $\alpha\text{-}Ni(OH)_{2(solid)} \rightarrow \beta\text{-}Ni(OH)_{2(solid)}$

4. Conclusions

In trying, you improve the capacity of the $NiO{\cdot}OH/Ni(OH)_2$ electrodes used in Ni–Cd, Ni–MH and Ni–Fe batteries, several modifications have been done to the nickel hydroxide microstructure. The capacity of the positive electrodes of $NiO{\cdot}OH/Ni(OH)_2$ depends on the microstructure of the precursor material [11]. The mechanism and the microstructure of the precursor material depend on the alkaline solution and nickel salt used in the synthesis. In the presence of NH_4OH solution as reagent, the synthesis of the nickel hydroxide occurs in five stages. The first one is the precipitation of nickel hydroxide for pH values between 8.0 and 8.6. The second corresponds to the formation of a complex such as $[Ni(NH_3)_6]^{2+}$, in the pH range between 8.6 and 10.0. The precipitation of nickel hydroxide happens again after pH 10.0. A layer of nitrate anions adsorbed on the solid makes difficult the exit of the water intercalated in the α-$Ni(OH)_2$. Therefore, a mixture of α-$Ni(OH)_2$ and β-$Ni(OH)_2$ phases is formed. In the presence of KOH solution as reagent, occurs the formation and ageing of nickel hydroxide. The chemical composition for nickel hydroxide can be expressed as follows: $[\beta\text{-}Ni(OH)_x(H_2O)_w(A^-)_y]$, where x, w and y are the amount of substance and A^- is the adsorbed anion.

Acknowledgements

The authors acknowledge PRPPG-UFES. Peter Baguley and Iara Baguley for manuscript revision.

References

[1] A. Shukla, S. Venugopalan, B. Hariprakash, J. Power Sources 100 (2001) 125.

[2] Y. Morioka, S. Narukawa, T. Itou, J. Power Sources 100 (2001) 107.
[3] J. McBreen, in: J.O.M. Brockris, B.E. Conway, R.E. Write (Eds.), Modern Aspects of Electrochemistry, vol. 21, Plenum Press, New York, 1990 (Chapter 2).
[4] P. Oliva, J. Leonard, J.F. Laurent, C. Delmas, J.J. Braconner, M. Fliglarz, F. Fievet, A. Guibert, J. Power Sources 8 (1982) 229.
[5] R.S. McEwen, J. Phys. Chem. 12 (1971) 1782.
[6] R. Archarya, T. Subbaiah, S. Anand, R.P. Das, Mater. Lett. 57 (2003) 3089.
[7] X. Liu, L. Yu, J. Power Sources 128 (2004) 326.
[8] X. Wang, H. Luo, P.V. Parkhutik, A.-C. Millan, E. Matveeva, J. Power Sources 115 (2003) 153.
[9] Q. Song, Z. Tang, H. Guo, S.L.I. Chan, J. Power Sources 112 (2002) 428.
[10] C.-C. Yang, Hydrogen Energy 27 (2002) 1071.
[11] M.B.J.G. Freitas, J. Power Sources 93 (2001) 163.
[12] Joint Committee on Power Diffraction Standards (JCPDS) Card No. 22-0444.
[13] Joint Committee on Power Diffraction Standards (JCPDS) Card No. 14-0117.
[14] K. Nakamoto, Infrared and Raman Spectra of Inorganic and Coordination Compounds, Wiley, New York, 1986.
[15] F. Potemer, A. Delahaye-Vidal, M. Figlarz, J. Electrochem. Soc. 133 (1992) 671.
[16] B. Mani, J.P. Neufville, J. Electrochem. Soc. 135 (1988) 800.